
METALLURGICAL SCIENCE AND TECHNOLOGY

A JOURNAL PUBLISHED
BY TEKSID
TWICE A YEAR

VOL. 19 No. 1, JUNE 2001

MICROSTRUCTURAL AND MECHANICAL EFFECTS OF LIQUID HOT ISOSTATIC PRESSING ON AA356 SAMPLES. I.

***M. E. Beghi, *G. Caglioti - **S. Barone, **C. Mus**
***Dipartimento di Ingegneria Nucleare, Politecnico di Milano**
Istituto Nazionale Fisica della Materia, Milano, Italy
****Teksid S.p.A., Borgaretto (Torino), Italy**

MICROSTRUCTURAL AND MECHANICAL EFFECTS OF LIQUID HOT ISOSTATIC PRESSING ON AA356 SAMPLES. I.

***M. E. Beghi, *G. Caglioti - **S. Barone, **C. Mus**
***Dipartimento di Ingegneria Nucleare, Politecnico di Milano**
Istituto Nazionale Fisica della Materia, Milano, Italy
****Teksid S.p.A., Borgaretto (Torino), Italy**

Abstract

Comparative tensile tests and microscopic images are reported of AA356 samples subjected to solubilization, quenching in water and T6 aging (*as cast*), and on samples of the same alloy subjected in addition, at the end of the solubilization period, to *Liquid Hot Isostatic Pressing (LHIP)*. LHIPing is a recent technical variant of conventional HIP-ing, where the pressure is transferred to the metallic components through molten salts rather than through a gas. Different solubilization times (1 ÷ 8 hours) at the temperature of 520 °C have been explored. The results confirm that, provided that the solubilization time exceeds 3 hours, LHIP-ing improves strongly the elongation to fracture and sensibly improves the ultimate tensile strength, UTS, practically without affecting yield.

In order to assess criteria for optimizing the casting process, the mechanisms of HIP-ing and their roles in the densification and the improvement of the ductility of the alloy are qualitatively analyzed for the specific heat treatments and LHIP parameters adopted in the present study.

Riassunto

Sono riportate prove di trazione uniassiale su campioni di lega AA356 sottoposti a trattamenti di solubilizzazione, tempra in acqua calda e invecchiamento T6 e immagini al microscopio di sezioni dei campioni stessi; i risultati sono confrontati con quelli relativi a prove su campioni della stessa lega sottoposti in aggiunta, subito dopo la solubilizzazione, a pressione isostatica a caldo (*Liquid Hot Isostatic Pressing LHIP*). LHIP è una recente variante tecnica dello HIP convenzionale, nella quale il trasferimento di pressione al getto metallico è assicurato da sali fusi anziché da un gas. Sono analizzati e discussi i risultati relativi a diversi tempi di solubilizzazione (1 ÷ 8 ore), alla temperatura di 520 °C. Le prove confermano che, se il tempo di solubilizzazione supera le 3 ore, LHIP-atura aumenta fortemente l'allungamento a rottura e migliora sensibilmente la resistenza a rottura, UTS, senza peraltro influire in modo rilevante sullo snervamento. Al fine di razionalizzare e, per quanto possibile, di quantificare i criteri correnti di ottimizzazione del processo di produzione di getti, anche alla luce dei risultati sperimentali sono analizzati i meccanismi di HIP-atura e il loro ruolo nella densificazione e nel miglioramento della duttilità, con riferimento specifico ai trattamenti termici e ai parametri di LHIP adottati nella sperimentazione.

1. OBJECTIVES

This contribution is part of a series of papers devoted to Liquid Hot Isostatic Pressure (LHIP) - a variant, developed by Teksid S.p.A. and Idra Presse S.p.A., of the traditional HIP densification process, where, perhaps for the first time, the external pressure is applied to the metallic components through molten salts rather than through a gas – [M. Rosso et al, 2000]. Its objective is twofold:

- To focus on the roles of the LHIP-ing parameters in both the densification of the porous structure of the *as cast* AA356 alloy under study and the improvement of its mechanical performance;

- To report and to compare the results of preliminary tests on the elongation to fracture and UTS of *as cast* vs. *as cast* + LHIP-ed samples, aimed at identifying optimal thermal treatments and LHIP-ing procedures.

2. THE MECHANICAL TESTS

64 heat treated sand cast samples have been submitted to standard tensile uniaxial tests.

32 samples (8 sets of 4 samples each) have been submitted to the following heat treatment: solubilization for 1, 2, 3 ... 8 hours in a salt bath at 520 °C, quenching in water at 65 °C, and T6 aging for 6 hours at 160°C.

The other (8 · 4 =) 32 samples, in addition, have been submitted also to LHIP: immediately after the solubilization treatment at 520 °C, while the sample temperature is still that selected for the solubilization

(corresponding to $0,85 T_m$, where $T_m = 933 \text{ K}$ is the melting temperature of the aluminum), isostatic pressures of the order of 115 MPa are applied for 35 s through molten salts.

In paragraphs 3. and 4. below the mechanisms of LHIP are examined with

3. MECHANISMS OF LIQUID HIP-ING: THE YIELDING STAGE AND THE DIFFUSION CONTROLLED STAGE

The density of a sand cast Al alloy component turns out to be generally smaller than the ideal one. The density reduction is mainly a consequence of the 6,5% reduction of the volume per unit mass of the alloy in passing from the liquid to the solid state: the tensile thermal stresses, created during the non-homogeneous cooling of the sample while it solidifies,

reference to optic macrographs and SEM micrographs of samples submitted and not submitted to LHIP. The results of the mechanical tests are presented in § 5.

We focus below on the densification produced by LHIP and the underlying mechanisms, in the neighborhood of the temperature and pressure values indicated in § 2. To this end, we refer to the classic works of J. Weertman and J.R. Weertman [1970], A.S. Argon [1966], M.F. Ashby [1990], and H. Exner and E. Arzt [1996].

The first two papers deal essentially with creep. The third and fourth papers, specifically dedicated to HIP and sintering, correlate the mechanisms of sintering promoted by high temperature and pressure to the mechanisms of creep promoted by high temperature and tensile stress; the approach of these last two papers is essentially that of interpreting HIP and creep in dual terms: HIP is envisaged as a kind of inverted creep.

During a creep test, in the bulk of the specimen under tensile stress (locally under 'tensile compression' or shear), the initial vacancy concentration increases toward values more and more removed from those at the thermodynamic equilibrium. As the tertiary, final creep stage is reached, necking is formed; in the necked region, vacancies coalesce lumping into submillimetric voids, and these voids grow to millimetric dimensions while the density diminishes catastrophically until fracture occurs.

As far as LHIP is concerned, the application of isostatic pressure to the cast component after solubilization produces two effects:

1. During the initial, yielding stage (stage I) -: an increase of the initial density via a reduction of the sizes of the pores.⁽¹⁾
2. During the final, diffusion controlled stage (stage II) -: the junction of the facing portions of the surfaces of the partially collapsed pores: a kind of local welding occurs, assisted by a drift diffusion ultimately promoted by the applied pressure.

As indicated above, after the solubilization treatment and prior LHIP-ing, the initial density of the quenched as cast samples already exceeds 96% of the ideal density. (Figs. 2 and 3). But since the void volume fraction due to the randomly

(1) In a fatigue or tensile test of an as cast solubilized and T6 aged sample not submitted to HIP-ing, the pores created during solidification act as cracks. The reduction of the pore sizes produced by (L)HIP during this Stage II., qualitatively accounts both for the sensible increase of the UTS reported in § 4 and discussed in § 5, and for the conspicuous increase of the number of cycles to rupture observed in fatigue tests which will be reported elsewhere (M. E. Beghi, G. Caglioti, S. Barone and C. Mus, to be submitted for publication, Metallurgical Science and Technology).

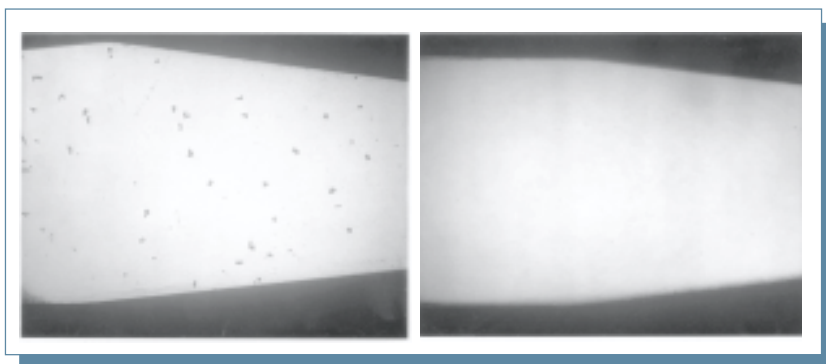


Fig. 1: Picture of the pore distribution in a longitudinal section of a) a sand cast sample and b) an as cast + LHIP-ed sample, heat treated as specified in § 2. Magnification: 5X. (Courtesy of Mr. Olimpio Di Tollo). The effect of the LHIP-ing process apparently is the collapse of the submillimetric pores

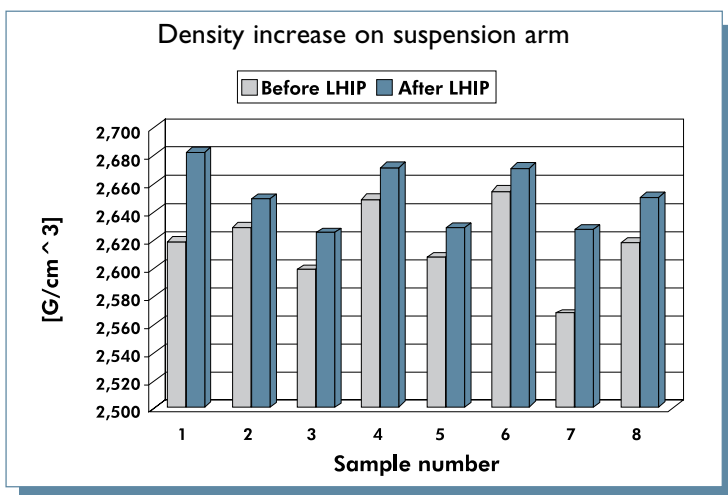


Fig. 2: Density of a set of sand cast AA356 Longitudinal Guided Arm (BLG) components submitted/not submitted to the LHIP treatment as specified in § 2

produce an essentially random distribution of pores throughout the bulk (Fig. 1). However the initial density never drops below 96% of the ideal density, neither for the series of the as cast tensile samples submitted to the mechanical tests described in the previous section (Fig. 2) nor for a set of sand cast Longitudinal Guided Arm (BLG) 936 automotive components (Fig. 3).

distributed submillimetric pores doesn't exceed the percolation threshold of 8% set by M.F. Ashby [1990], the pores are sealed off. The macrographs in Fig. 1 confirm that under these topological conditions no percolation toward the external surface could favor densification during (L)HIP-ing. Furthermore the very presence of these submillimetric pores in the as cast samples suggests that the concentration of vacant sites in the bulk of the untreated samples exceeds by several orders of magnitude the equilibrium concentration.

3.1 STAGE I.

At the beginning of (L)HIP-ing, under a local pressure P_{lim} much larger than the yield stress at the solubilization temperature, the pores shrink rapidly. According to Ashby this local pressure, "high enough to cause yielding of the spherical shells surrounding each pore" is given by:

$$(I) \quad P_{lim} = \frac{2\sigma_y}{3} \cdot \ln \left[\frac{l}{l - A_{yield}} \right],$$

where A_{yield} is the level attained by the density of the alloy at the end of the yielding stage (stage I). The histograms in figures 2 and 3 show that in the operating conditions of § 2., the average value of A_{yield} falls in the range (0,985 ÷ 0,996). According to eq. (I), the lower limit of the local pressure, P_{lim} , required for the pore collapse, increases mildly with the densification level attained by the alloy, and doesn't exceed 10 MPa, a value roughly three times larger than the yield stress of the alloy at the solubilization temperature. This threshold of the local pressure turns out to be about ten times smaller than the applied external pressure, whose value is selected in the 100 MPa range by the press producer.

This comparatively large value of the applied pressure is more than sufficient to promote promptly the pore collapse observable when Figures 1 a) and 1 b) are compared.

The densification induced during stage I. of LHIP can be perceived also comparing the macrographs of Figures 4 a) and 4 b).

Finally, the same trend can be recognized once more, examining the micrographs of the fracture surfaces of not LHIP-ed and LHIP-ed samples in Fig. 5 a) and 5 b) respectively. Although even for the LHIP-ed sample the density of the pores intersecting the fracture surface largely exceeds the average pore density in the bulk (responsible for the aforementioned void volume fraction of the order of 1%), the sizes of the pores in the

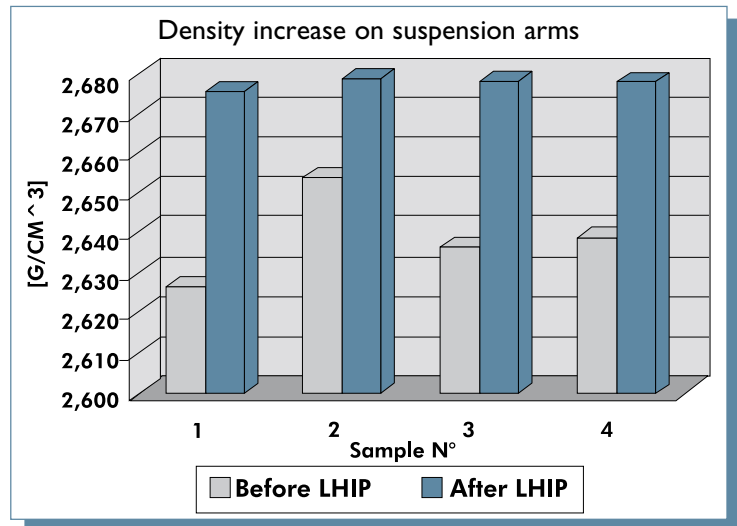


Fig. 3: Density of a set of sand cast AA356 Longitudinal Guided Arm (BLG), 936 components submitted/not submitted to the LHIP treatment as specified in § 2

neighborhood of the fracture surface are much smaller for the LHIP-ed samples than for the not LHIP-ed one's. The residual difference between the actual density of the LHIP-ed samples, in the range (0,985 ÷ 0,996 % of the ideal density), and the ideal density ($2,685 \cdot 10^3 \text{ Kg m}^{-3}$) could be due to the excess of vacancies in non-equilibrium in the quenched samples and the hydrogen yet dissolved in the bulk.

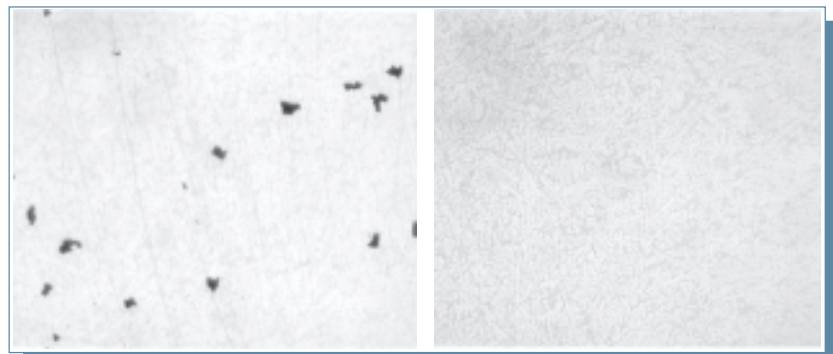


Fig. 4: Picture of the pore distribution in a chemically etched longitudinal section of a) a sand cast sample and b) an as cast + LHIP-ed sample, heat treated as specified in § 2. Magnification: 10X. (Courtesy of Mr. Olimpio Di Tollo). While it is confirmed that LHIP-ing promotes the collapse of the submillimetric pores, the chemical etching reveals the dendritic nature of the microstructure

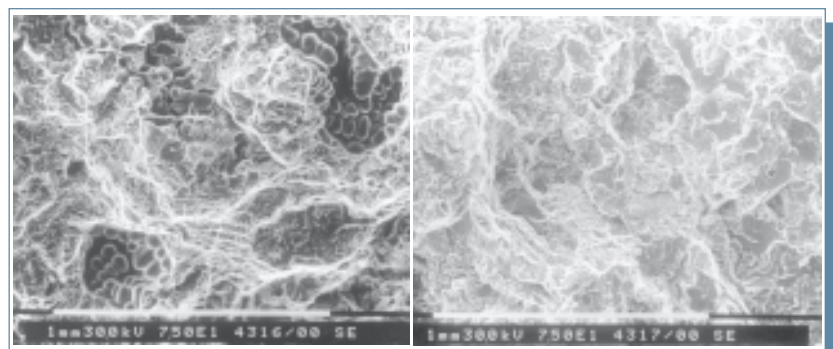


Fig. 5: Micrographies of the structure of the pores intersecting a fracture surface for a not-LHIP-ed sample a), and for a LHIP-ed sample b). (Courtesy of Mr. Olimpio Di Tollo). A consequence of LHIP is the healing of the dendritic branches, at the micrometric scale

3.2 STAGE II.

Only few seconds after the application of pressure, LHIP-ing enters the final stage. Although the densification achieved by local yielding is immediately completed during the short time allotted to stage I, at this point the facing portions of the folded surfaces of the collapsed pores could yet be envisaged as thin cracks hampering the mechanical performance of the alloy. However an important process should start now: a sort of welding of the facing portions of the squashed pores brought into contact during stage I., promoted at this point by thermally activated and pressure-assisted local diffusion.

The mechanism underlying this process should be essentially the same as the mechanism described by H. E Exner and E. Arzt [1996], responsible for the nucleation and growing of necks at the junction between initially loosely packed particles during sintering. According to these Authors, the pores act as vacancy sources or atom sinks for the surrounding particles: the atoms diffuse along and across the boundaries of the crystal grains; and their diffusion is "enhanced in hot-pressing because the additional energy $\sigma\Omega$ is gained on moving an atom with volume Ω from the interparticle boundary which is acted on by a compressive traction σ into the pore space or to the surface". This compressive traction – essentially a shear stress – should arise, even if the applied pressure originating it is globally isostatic, as a consequence of the irregular shapes of the pores: geometric irregularities lead to anisotropy in the local redistribution of the external stress. A dual statement equivalent to that one quoted above could be: the vacancies diffuse along and across the boundaries of the crystal grains; and their diffusion is enhanced in hot-pressing because the additional energy $\sigma\Omega$ is gained on moving a vacancy with volume Ω from the surface of the pore space into the interparticle boundary which is acted on by a tensile compression σ .

Therefore, as remarked above, although the densification promoted by local yielding is completed, the collapsed pores could still hamper the mechanical performance of the alloy if they were not healed up due to the Al atom diffusion toward the pores and/or the vacancy diffusion toward the bulk. This dual diffusion process can be envisaged as a drift-self-diffusion enhanced by the shear stresses s originated locally by the applied *isostatic pressure*; it leads to the healing of the pores, whose linear dimensions are now reduced to few tens of micrometers.

According to Ashby, if the grain size G is smaller than the size of the particles, the HIP-ing is controlled mainly by volume diffusion (Nabarro-Herring creep). To a minor extent, at high temperature, grain boundary diffusion (Coble creep) contributes also to HIP-ing. The following rate equation for the diffusion flow is then proposed [Ashby 1990, eq. (36)]:

$$(2) \quad \frac{d\varepsilon}{dt} = \frac{14 \sigma \Omega}{KT} \cdot \left[\frac{D_v}{G^2} + \frac{\pi \delta D_b}{G^3} \right],$$

where K is the Boltzmann constant, D_v and D_b are the volume and the grain boundary diffusion coefficients, δ and G are the grain boundary thickness and grain size respectively. In the numerical estimates we will neglect the contribution to the Coble creep. (Should power law creep conditions dominate, the linear dependence would be substituted by a power law of $\sigma\Omega$).

Since the self diffusion is a thermally activated process, the kinetics of the densification is enhanced *exponentially* by the thermal energy and

controlled *exponentially* by the activation energy for vacancy diffusion or atomic self diffusion. The driving factor, $14 \sigma\Omega/(KT)$, depends *linearly* on the work $\sigma\Omega$ of the local shear force promoting an atomic displacement of the order of the atom size.

The atoms responsible for the strain rate of eq. (1), diffusing from a grain contiguous to a partially squashed pore toward the facing portions of its folded surfaces, produce a kind of junction of these surfaces ultimately promoted by the applied pressure. Their drift velocities $\langle v \rangle$ is:

$$(3) \quad \langle v \rangle = \frac{14 \sigma \Omega}{KT} \cdot \frac{D_v}{G}.$$

4. EFFECTS OF LHIP ON THE DEFECTIVE MICROSTRUCTURE OF THE SAMPLES UNDER STUDY

In this paragraph equations (2) and (3) are utilized in order to account for the evolution of the microstructure promoted by the action of LHIP on the AA356 samples analyzed in the present investigation.

In Fig. 4 the dendritic nature of the structure of our samples is evidenced. Dendrites grow during any diffusion limited aggregation (DLA) process. The DLA develops during solidification provided the controlling parameters – local temperature gradients, surface tension and local curvature of the solidifying front – happen to lie in specific intervals. DLA is characterized by a sequence of elementary steps promoted at the atomic scale by the systematic, recurring application of the same set of rules. A natural consequence of the *systematically repeated application of the same set of rules* is that the pattern produced by the process exhibits the feature of being *statistically invariant* against a change of scale: each part of the structure turns out to be a copy of a part of the structure and eventually of the entire structure: the structure exhibits the statistical selfsimilarity typical of the fractals [see e.g. T. Viksek, 1986].

No wonder if the dendritic nature of the structure remains evident not only in the macrographs of Fig. 4, but also in the micrograph of fig. 5 a), showing details of the internal surface of the pores intersected by the fracture surface of a sample which was not LHIP-ed. The appearance of the pore surface changes drastically

when the alloy is LHIP-ed: at the microscopic level ($\sim 30 \div 50 \text{ nm}$) the boundaries between contiguous dendritic protuberances disappear. Eqs. (2) and (3) are helpful to account for the LHIP induced healing of the dendritic branches at the micrometric scale, provided that we interpret the grain size diameter G as the average linear dimension of the microscopic dendritic protuberances.

Setting:

- $\sigma \sim 100 \text{ MPa}$,
- $\Omega = 12 \cdot 10^{-30} \text{ m}^3$ (the vacancy volume is estimated equal to the volume of an aluminum atom in the crystal),
- $D_v = 6 \cdot 10^{-13} \text{ m}^2/\text{s}$,⁽²⁾
- $G \sim 5 \cdot 10^{-5} \text{ m}$,

one gets for the drift velocity of the atoms $\langle v \rangle$ the following order of magnitude:

$$(4) \quad \langle v \rangle \sim 2 \cdot 10^{-8} \text{ m/s.}$$

During the duration time $t = 35 \text{ s}$ of stage II, the atoms migrate along and across the boundary between adjacent protuberances by distances of the order of

$$(5) \quad \langle v \rangle t \sim 0.7 \text{ } \mu\text{m.}^{(3)}$$

Since the thickness of the boundaries between contiguous dendritic protuberances is indeed of the order of $1 \text{ } \mu\text{m}$, we believe that the fact that the internal surfaces of the pores lose their dendritic appearance should be attributed to the LHIP assisted local diffusion promoting a kind of local welding of contiguous protuberances.

In conclusion, the fracture surface of the LHIP-ed sample exhibits fewer pores of very reduced dimensions, whose internal surfaces don't exhibit any more pronounced dendritic features, in agreement with the above considerations.

(2) This value is derived from J.L. Bocquet et al. (1996), p. 575. It refers to the alloy in thermodynamic equilibrium. However since selfdiffusion is associated to a vacancy diffusion mechanism and since in the not LHIP-ed samples the vacancy concentration largely exceeds the equilibrium concentration, the numerical values of the strain rate (Eq. (3)), of the average atomic drift velocity (Eq. (4)) and of the atomic displacements along and across the interdendritic protuberances (Eq. (5)), should be sensibly underestimated.

(3) Traces of gases dissolved in the ingot could slightly modify the above picture. At high temperature the oxygen, in the presence of water vapor, reacts with the aluminum producing alumina, and liberates hydrogen. At atmospheric pressure the hydrogen solubility in liquid aluminum does not exceed $1 \text{ cm}^3 / 100 \text{ g Al}$. In practice the hydrogen concentration in the solid is usually confined in the range $(0,07 \div 0,4) \text{ cm}^3 / 100 \text{ g}$. These values are more than sufficient to produce supersaturation of this gas during the solidification at ordinary temperatures, and could be partly responsible for the lower than ideal density of the solubilized alloy. The hydrogen could accumulate preferentially in the pores; but since the atomic size of the hydrogen is much smaller than that of the aluminum atom, most likely, during solubilization and LHIPing, hydrogen diffuses interstitially in the bulk, distributing homogeneously in it.

5. RESULTS OF THE MECHANICAL TESTS

The experimental tests described in § 2 lead to the following results:

1. The process of LHIP-ing promotes an increase of the elongation to fracture, from 0.6 % to 3.0 %. Below a solubilization time of 3 hours at $520 \text{ }^\circ\text{C}$, LHIP-ing is ineffective;
2. The process of LHIP-ing promotes also an increase of the ultimate tensile strength, UTS, from 210 MPa to 250 MPa, again provided that the duration of the solubilization time exceeds 3 hours.
3. The process of LHIP-ing seems to promote also a slight increase of the yield stress, $\sigma_{0,2}$, - from about 203 MPa to 213 MPa -, barely exceeding the experimental error.

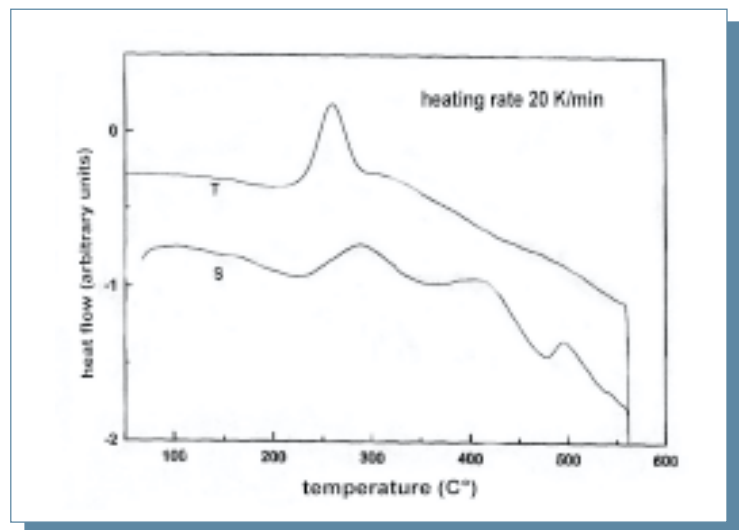


Fig. 6: DSC diagrams for two samples T and S of the AA356 alloy described in the text.

6. DISCUSSION AND CONCLUSIONS

The experimental results exhibit a conspicuous improvement of the elongation to fracture for the LHIP-ed samples in comparison with the as cast ones.

This finding is coherent with the results obtained by other Laboratories for the same alloy submitted to other casting processes characterized by the application of a pressure while casting proceeds. For instance, P.A. Karnezis, et al. [1996] report an increase by a factor eight of the elongation to fracture of the squeeze cast and the roll cast alloy with respect to the gravity cast (Table 1).

TABLE 1. MECHANICAL PROPERTIES OF THE AA356, SOLUBILIZED AT 540°C FOR 12 HOURS AFTER CASTING, QUENCHED IN HOT WATER AND AGED AT 155°C FOR 12 HOURS (FROM REF. 2)

	0.2% proof stress, MPa	UTS, MPa	Elongation, %
Gravity cast	246 ± 11	278 ± 7	0.9 ± 0.2
Squeeze cast	253 ± 5	320 ± 3	7.6 ± 0.5
Roll cast	229 ± 6	293 ± 7	7.7 ± 0.1

These Authors attribute the above results to the reduction of the number and sizes of the pores, promoted by the applied pressure.

The values reported in Table I suggest that there is plenty of room for further improvement of the elongation to fracture of the alloy under study.

From the findings of paragraphs 3 and 4, the LHIP-ing time seems to be sufficiently long for the healing of the dendrites at the microscopic scale. Evidence for the beneficial effect of the healing of the dendrites on the mechanical properties of interest in the present study is reported in G.I. Eskin [1998].

Remarkable advantages are expected from the adoption of higher values of the solubilization temperature.

In particular, in order to assess the maximum value of the solubilization temperature, which could be safely adopted without damaging the alloy provided that it was possible to exert an ideally accurate temperature control not only in the laboratory but also during production, two samples of the AA356 alloy described below have been subjected to tests of Differential Scanning Calorimetry (DSC), aiming to measure the minimum melting temperature of the eutectic:

Sample T. As cast, cooled as fast as possible till 400°C, kept at this tem-

perature for about 1 minute while being removed from the die, quenched in water and stocked in freezer before testing;

Sample S.As cast, cooled till 400°C, removed from the die, air cooled, solubilized at 540° for 8 hours, quenched in water and stocked in freezer before testing.

Notwithstanding the quite different thermal treatments experienced by these two samples, a unique common feature is evident from the DSC diagrams of Fig. 6: *the minimum melting temperature of the eutectic*, whose value, for both, *doesn't drop below 563 °C*. This temperature is much higher than the solubilization temperature of 520 °C explored so far.

Further tests will be performed in order to ascertain the effects of higher solubilization temperatures according to the aforementioned practical constraints and DSC results.

7. ACKNOWLEDGMENTS

We are grateful to Professor Sergio Gallo for his advice and stimulating discussions. We thank Professor M. F. Ashby for having made available to us his Technical Report *HIP 6.0*, Cambridge University, U.K. (1990), and Professor Giuseppe Riontino of the Università di Torino for his DSC tests.

Thanks are due to Mr. Antonio Mantegazza (Politecnico di Milano) for his assistance in the mechanical tests, and to Mr. Olimpio Di Tollo of the Centro Ricerche Fiat Orbassano, for his work at the optical and the scanning electron microscopes.

REFERENCES

1. M. Rosso, C. Mus, and G. Chiarmetta, Liquid Hot Isostatic Pressing process to improve properties of thixoformed parts, *Metallurgical Science and Technology*, 18, N° 2, pp. 16-18 (2000)
2. P.A. Karnezis, G. Durrant and B. Cantor, Effects of Processing on the Microstructure and Tensile Properties of A356SiC_p MMCs, *Materials Science Forum* Vols. 217-222 (1996) pp.341-346
3. J.Weertman and J.R.Weertman (1970), Mechanical Properties Strongly Temperature Dependent, in *Physical Metallurgy*, Second revised edition, ed. R. W. Cahn, North Holland, pp. 985-1010
4. A. S. Argon (1996), Mechanical Properties of Single-Phase Crystalline Media: Deformation in the Presence of Diffusion, in *Physical Metallurgy*, Third edition, Eds. R.W. Cahn and P Haasen, Elsevier, pp. 1958-2007
5. J.L. Bocquet, G. Brebec and Y. Limoge, Diffusion in Metals and Alloys in *Physical Metallurgy*, 4-th revised edition, R.W. Cahn and P Haasen Eds., Elsevier Science, (1996) Ch. 7
6. M. F. Ashby (1990), *HIP 6.0: Background Reading, Sintering and Isostatic Pressing Diagrams*, Technical Report, Department of Engineering, University of Cambridge
7. H. E. Exner and E. Arzt (1996), Sintering Processes, in *Physical Metallurgy*, 4-th revised edition, R.W. Cahn and P. Haasen Eds., Elsevier Science, (1996).
8. T. Vicsek (1986), Formation of Solidification Patterns in Aggregation Models, in *Fractals in Physics*, Eds. L Pietronero and E. Tosatti, North Holland, Amsterdam, pp. 247-250
9. G.I. Eskin, *Ultrasonic Treatment of Light Alloy Melts*, Gordon and Breach Science Publishers, 1990